Project Title: Low-Cost, Reliable Soft Arm for Robotic Tree Fruit Operation Phase II

Report Type: Final Project Report

Primary PI: Ming Luo
Organization: Washington State University, School of Mechanical and Material Engineering
Telephone: 509-335-4034
Email: ming.luo@wsu.edu
Address: Sloan 211
Address 2: 405 NE Spokane st
City/State/Zip: Pullman, WA 99163

Co-PI 2: Manoj Karkee
Organization: Washington State University, Center for Prec. & Automated Ag. Systems (WSU CPAAS)
Telephone: 509-786-9208
Email: manoj.karkee@wsu.edu
Address: 24106 N Bunn Rd
Address 2:
City/State/Zip: Prosser, WA 99350

CO-PI 3: Matthew Whiting
Organization: Washington State University, Center for Prec. & Automated Ag. Systems (WSU CPAAS)
Telephone: 509-786-9260
Email: mdwhiting@wsu.edu
Address: 24106 N Bunn Rd
Address 2:
City/State/Zip: Prosser, WA 99350

Cooperators: Dave Allan, Allan Brothers Fruits; Deb Pehrson, Tim Welsh, Columbia Orchard Management, Inc.; FFRobotics, Israel

Project Duration: 2-Year

Total Project Request for Year 1 Funding: $ 106,029
Total Project Request for Year 2 Funding: $ 110,010

Other related/associated funding sources: None
Funding Duration:
Amount:
Agency Name:
Notes:
WTFRC Collaborative Costs: None

Budget 1
Primary PI: Ming Luo
Organization Name: Washington State University
Contract Administrator: Anastasia Mondy
Telephone: (916) 897-1960
Contract administrator email address: arcgrants@wsu.edu
Station Manager/Supervisor:
Station manager/supervisor email address:

Item	2023	2024	(Type year start date of year 3 here if relevant)
Salaries	$51,618.00	$53,683.00	
Benefits	$9,718.00	$10,106.00	
Wages	$23,314.00	$24,246.00	
Benefits	$2,379.00	$2,475.00	
RCA Room Rental			
Shipping			
Supplies	$8,500.00	$8,500.00	
Travel	$10,500.00	$11,000.00	
Plot Fees			
Miscellaneous			
Total	$106,029.00	$110,010.00	$216,039.00

Footnotes:

Abstract:
Washington state tree fruit growers face labor shortages for tasks like harvesting and pruning, leading to significant investment in robotic solutions. Our team has developed a soft-growing manipulator, featuring a 2.46 ft fabric arm with adjustable speed (1.23 ft/s extension, 0.86 ft/s retraction) and a 2.39 lbs. payload. The spherical-shaped workspace, low-cost ($4,404) system navigates orchards without damaging fruit or branches. For harvesting operations, we have developed a soft-gripper end-effector tool that utilizes silicone rubber and flexible plastic to safely and firmly grasp fruit. The current design has a successful pick rate of 87.5% and is low-cost at around $59. We have also developed a global and local camera and machine vision system to detect apples within the system's workspace and to obtain the real-time position of the end-effector with respects to target apples. The apple detection system has a mean average precision value of 0.98 and a confidence percentage of >70% for detected apples. Currently, the camera system uses a QR code to detect the position of the end-effector, and we are working on a localization system that uses the global and local cameras with the detected apples to find the end-effector position. These systems also include depth sensing to provide additional measures of accuracy and are easily removable to adapt the system to the desired purpose. We have also designed and implemented an adaptive controller into the system providing desirable behavior and allowing for the compensation of added payloads. The entire system has been experimentally verified in a lab setting. Following lab tests, we demonstrated the system in a commercial orchard and plan to fully integrate components in the next phase for comprehensive field evaluation.

Key Words:
Soft Robotics, Robotic Harvesting, Orchard Safety.

Objectives:

Objective#1: Design, fabricate, test, and optimize a growing arm/manipulator for orchard operations (Luo – Lead, Karkee – Co Lead;)

Overview in the proposal: To perform various field operations in tree fruit production, our soft growing manipulator will have the following mechanical features: 1) 4 ft radius workspace - the proposed manipulator length (4 ft) is expected to cover the entire tree height (~8ft) when installed on a ground platform that is approximately half of the tree height. 2) Free movement in 3D space with up to 3 lbs. payload (which is sufficient to carry most of the end-effectors such as a fruit picker or an electric scissors for pruning) - Our proposed manipulator must overcome gravity to grow, retract, and steer to reach any target within its workspace. 3) Ability to maneuver freely inside most tree canopies under 8 ft height: The diameter of our proposed manipulator and updated design of end-effector adaptor/mount allows the manipulator to pass through narrow spaces between branches.

Our current achievement:

- Length: Can extend up to 2.46 ft reliably with a high degree of control.
- Speed: Manipulator displays 1.23 ft/s growing speed and 0.86 ft/s retraction speed at 8 and 3 psi of pressure respectively. We have observed that higher pressures and airflow rates result in dramatically faster extension speeds. Currently, the speed is limited by the airflow rate and the free spin speed of the central motor.
- Targeting Speed: The manipulator can reach a point near the edge of its workspace from its default position with a target rise time of 1.28 seconds and a settling time of 3.30 seconds with less than 0.04 in of steady-state error.
- Payload: 2.39 lbs. payload at 10 psi pressure input while at the max arm length. This payload includes the weight of the tip mount, soft-gripper, and fruit. With the tip mount and gripper being under 1.75 lbs., there is sufficient payload to carry an apple under 0.64 lbs.
- Workspace: One RealSense D456 camera is able to detect 3D position in 6 by 3 ft range at a 3 ft depth with a high degree of accuracy. Our robot's optimal workspace has a spherical sector shape with a radius of 2.5 ft and 60 degrees of actuation in the 2D plane, providing a total workspace volume of 22.46 ft^3.
- Pressure Reliability: The maximum input pressure of our fabric material's sealing is above 20 psi, and 5-10 psi is our operation pressure range since it displays adequate payload and control properties. In addition, there is a pressure relief valve to reduce the risk of pressure overloading.
- System Reliability: The system can operate for prolonged periods of time, >2 hour, without noticeable changes in control performance or degradation due to the system design.
- R&D cost: The current prototyping cost ($) of a single manipulator is eight times less than a commercially available rigid manipulator. The estimated cost is approximately $4,404, which is broken down into $574 for materials, $547 for manufacturing, $2,474 for electronics, and $809 for other mechanical components. The most expensive part is the central motor, which costs $1,117. Due to the urgent timeline, we purchased an expensive and powerful motor to verify our system first. We believe we can find an alternative item under $100 when system verification is done, and the overall cost will be approximately $3000 at the commercial manufacturing stage.

Objective#2: Manipulator integration with a low-cost machine vision system and selected end-effector tools (e.g. for picking, year 1) (Karkee – Lead, Luo – Co Lead).

Overview in the proposal: To prototype a robotic system for field testing with various operations, we will develop a perception system and integrate it with the soft, growing manipulator. In addition, a commercially available cable driven soft gripper will be integrated (one at a time) with the end-effector mount (Obj # 1) to support apple harvesting use case.

Our current achievement:

- Machine Vision Model: The current YOLOv8 model trained on the images of apples taken in the Allan Bros Orchards in Prosser, WA with the local and global cameras mounted on the soft robotic manipulator has an apple detection accuracy of 98%.
- Image Based Visual Servoing (IBVS): Two cameras are used to estimate the real time positions of the end-effector and detected apples using a QR code mounted onto the end-effector and the machine vision model respectively. The global camera uses eye-on-hand configuration of visual servoing while the local camera uses eye-in-hand configuration to manipulate the end effector on the end goal.
- Image-Based Localization: The cross image-based localization used to find the end-effector position utilizes images from both local and global cameras to detect apples, find correlated apples, and determine the displacement between camera frames with some level of distortion between images to determine end-effector location. The vision system is flexible for various requirements in its application.
- Gripper Efficacy: The soft gripper with a thermoplastic polyurethane (TPU) 3D-printed endoskeleton can grasp apples without causing damage to the fruit. This gripper end-effector has achieved a successful pick rate of 87% in a field test during the 2023 harvesting season.
- Gripper Design: A secondary servo motor and gear system allows the entire gripper to twist, simulating the twisting motion of a human worker.
- Gripper Weight: The gripper is lightweight at 0.91 lbs. and can be mounted to the soft manipulator arm without exceeding the payload limit.
- Gripper Cost: Given the current design that does not require costly sensors, the price of one soft gripper unit stands at approximately $59.

Objective#3: Design and implement a low-level controller to achieve automated operation (Luo – Lead, Whiting – Co-Lead).

Overview in the proposal: Once the perception/vision system, end-effector tool (Obj#2) and soft manipulator (Obj#1) have been tested separately for their functionality, they will be integrated together for overall system evaluation in the simulated, laboratory environment as well as in the field environment using automated motion/control techniques discussed below.

Our current achievement:

- The current system is controlled using a Model Reference Adaptive Controller (MRAC) that utilizes the system's dynamical data to reliably control the arm to follow a desired behavior.
- For a given end point within the system's workspace the manipulator displays a target rise time of 1.28 seconds, a settling time of 3.3 seconds with less than 0.04 in of steady-state error. The control of the system can be improved by using faster and more powerful steering motors, as they will allow for a faster reference model to be used in the system's controller.
- The system control can reliably compensate for additional payloads up to 1.21 lbs. without significant impact to the system's behavior.

Overall progress

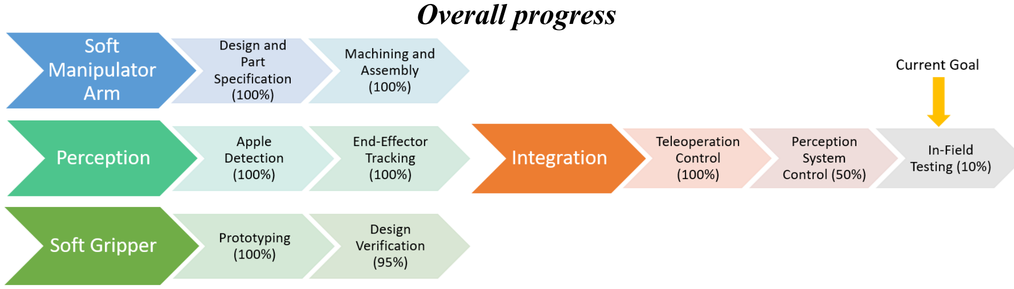

Figure 1. Goals vs. current progress.

Significant Findings:

Objective#1:

- The maximum operating pressure of the system depends on the maximum pressure of the fabric arms. So far, tests have shown that the fabric arms are capable of withstanding 20 psi. Thus, we can safety and reliably operate at or below 10 psi, which is sufficient for apple harvesting.
- The fabric arms display a high life-span and durability, only failing after prolonged use, user caused pressure spikes, or system control failure.
- The growing and retracting speeds are primarily affected by the airflow rate in and out of the system as well as the air pressure.
- The configuration of the steering motors impacts the system's ability to compensate for the effects of gravity on the fabric arm.
- A well-made closed-loop controller can compensate for positional errors caused by the pulley diameters changing when material is spooled and unspooled during operation.
- The mathematical model of the system is relatively accurate for a soft robot platform.
- The system parameters, azimuth angle, elevation angle, and fabric arm length, are dependent on each other despite being controlled by separate mechanisms.
- The steering buffer increases the reliability, consistency, and range of the system control.
- Placing the central motor outside of the enclosure prevents overheating and electrical issues.
- The friction from the end-effector mount has a significant impact on the speed of growing and retraction. The current design of the mount dramatically reduces this friction.
- The power requirements for using stronger brushless motors and higher pressures can be accounted for by using robust power supplies or high-power batteries.

Objective#2:

- Image-based localization responds well with singular frames rather than video feeds.
- The detection system can detect apples in varied outdoor lighting conditions with a mean average precision (mAP) value of 0.98. The vision system considers detection significant if the confidence threshold is greater than 70%.
- In scenarios where a bright light source is present in background or in plane of detections, the detection accuracy reduces significantly. High dynamic range (HDR) correction as a post process needs to be added in vision pipeline, in order to avoid this behavior.
- Both global and local camera based visual servoing are running simultaneously with distance error as low as 1.18 in.
- At high fps data (>25 fps) in outdoor conditions, that multi camera feed halts.
- Embedding a flexible but stiff thermoplastic skeleton into the silicone fingers of the soft gripper dramatically improves the picking rate.
- Found a successful pick rate of 87% for our gripper during picking efficacy experiments conducted in the 2023 harvesting season.
- Including a metal bolt as the soft gripper's pulley significantly improves the integrity and reliability of the soft gripper.
- Adding a secondary servo motor allows for a twisting motion to simulate a human worker.
- Design changes kept the overall weight of the soft gripper end-effector to under 1 lbs., thereby meeting the payload requirements.

Objective#3:

- The combined parameter controller provided significantly better performance compared to the split parameter controller due to the improved mathematical model.
- Introducing feedforward terms generated from the mathematical model caused undesirable amounts of overshooting. Compensating for this overshooting resulted in making the controller unstable or slow to respond.

- Implementing a model reference adaptive controller (MRAC) significantly improved the system's performance by making all system parameters follow a desired behavior, resulting in minimal distance covered and all parameters converging simultaneously.
- The MRAC allows for consistent control behavior regardless of additional payloads.
- Due to the system's design and control, it can be easily teleoperated within the lab and orchard environments without damaging the trees, fruit, or the robot body.

Methods:

Objective#1:

Growing and Retracting Speed Testing: The growing and retraction speeds were determined by using motion-tracking cameras and markers to record the position of the arm while it moved. For growing speed, the arm was allowed to freely grow while the system was held at 8 psi. For retraction speed, the central motor pulled on the fabric arm as fast as it could while the system was set to 3 psi. From these processes, the growing and retracting speeds were found to be 1.23 ft/s and 0.86 ft/s respectively. These speeds can be further increased by using a more powerful central motor, as higher pressures can be used during growth, and faster speeds can be used during retraction. While more powerful motors may increase the cost, the central motor drastically impacts the performance of the system. Therefore, the benefits of a more powerful motor outweigh the costs.

Fabric Arm Pressure Testing: The heat sealing of the fabric arms with the new material was verified by testing three small fabric arms. These fabric arms were around 1.3 ft in length. The fabric arms were attached to a pressure testing setup where the internal pressure applied to the arms slowly increased from 0 to 20 psi. All the arms tested survived the pressure testing up to 20 psi without any significant damage to the heat-welds. Pressures beyond 20 psi were not tested as the pressure testing setup was designed for a max operating pressure of 20 psi. This process demonstrated that the fabric arms can reliably operate at higher pressures without failing. Thus, while at our operating pressure range of 5 to 10 psi, the fabric arms are significantly more reliable, last longer, and are more durable.

Manipulator Arm Payload Testing: The maximum payload capabilities of the manipulator arm were evaluated while at its full straight arm length of 2.46 ft and under constant pressure. In this test, 0.01 lbs. weights were incrementally added until the combined weight of the end-effector mount and the added weight caused the arm to buckle or sag uncontrollably. This total weight was then considered to be the maximum payload for the given air pressure setting. This process was repeated for pressures ranging from 2 to 10 psi in 1 psi increments and then the entire testing procedure was repeated two more times to account for possible errors. From this test, the maximum payload of the arm at 10 psi was found to be 2.39 lbs. or 70.55 in-lbs., shown in Figure 2. Overall, this test displays more than sufficient payload capabilities for apple picking, as the maximum payload of 2.39 lbs. can easily support the end-effector mount, soft gripper, and a large apple up to 0.64 lbs. With stronger fabric arms, improved manufacturing capabilities, better pressure systems, and a more powerful center motor this payload capacity can be further improved. Thereby increasing the robustness of the system and enabling greater use in the orchard environment.

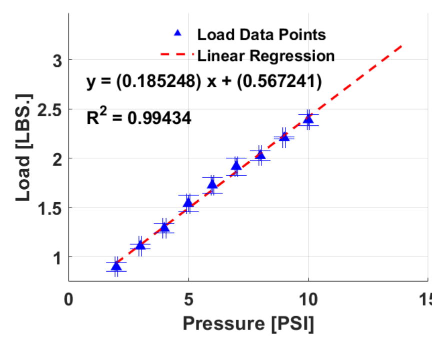

Figure 2. Plot of the max payload capacity at the max arm length.

Objective#2:

Gripper Harvest Testing: During the 2023 harvesting season, the prior gripper prototype was tested in a practical orchard setting. The test was performed at the Allan Brother's orchard with the Envy apple variety. The reliability of the gripper, maneuverability within the tree canopy, and the rate of successful picks performed was evaluated. Using thin fingers, the gripper was able to successfully wrap around apples with minimal interference from obstacles such as neighboring apples, branches, and leaves, shown in Figure 3. Three different types of printing patterns were tested for the embedded TPU skeleton. Around 40 apples were picked using each of the finger types, totaling 120 apples.

Figure 3. Gripper approaching, encompassing, and picking apple.

Machine Vision Testing: The machine vision system uses a localization algorithm based on our trained YOLOv8 model for apple detection. The system was tested in a lab setting with known apple positions relative to the cameras. Localization testing involved varying the end-effector angle relative to the in-lab trees while keeping the global camera in a fixed position. During testing, the detection results were found to differ based on input type (video or image) and on the angle and distance between cameras. Detection performed best from image feeds, with image clips captured by cameras at 90 Hz.

Visual Servoing Testing: After obtaining the 3D position of the target apple, two vision systems are used to determine the 3D position of the tip mount and its relative position to the targeted apples. Currently, the tip position system uses a QR code identifier attached to the tip mount and the global camera while the relative apple position system utilizes both local and global cameras. The visual servoing in-lab test setup consists of the global camera mounted on the manipulator base, the local camera mounted on the end effector along with the QR code, and a stand-in apple, shown in Figure 4. This setup enables real-time visual servoing at 30 Hz using the open-source ROS package VISP. By calculating the error vector between the robot tip and target apple positions, the robot can be guided to the desired location. Current work focuses on implementing additional sensors, such as an IMU, to enhance accuracy and reduce sensor drift. Future work aims to remove the QR code and solely use localization algorithm with the local camera embedded in the palm of the soft gripper.

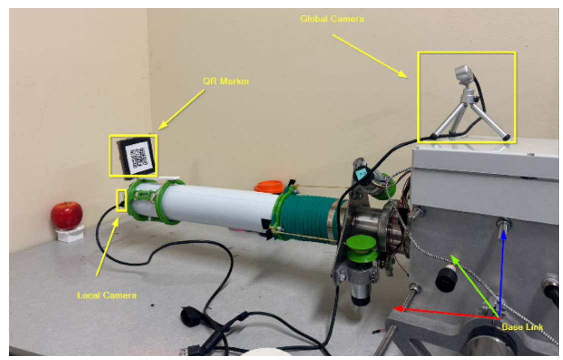

Figure 4. Experimental setup for validating the machine vision and visual servoing systems.

Objective#3:

Workspace Testing: The workspace of the system was verified by using the improved mathematical model to complete two different workspace evaluation tests. Both tests used open-loop control, just the mathematical model, to drive the arm to the desired position. The first test had the arm follow three different circular paths within the system's workspace. Each path utilized the same arm length but used a different pitch angle at the base of the arm. The 3D positional data of the tip of the end-effector mount was collected using a motion capture camera system, as seen in Figure 5. From this test, the paths that the arm made using solely the mathematical model were relatively close to the desired paths and resembled a spherical sector shape. The second test had the arm drive to several

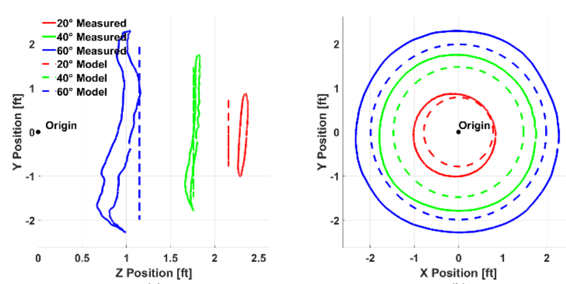

Figure 5. 3D positional data compared to the path specified by the mathematical model.

distinct points within the system's workspace. These points were defined by a set of arm steering angles for three different arm lengths. The final position was then compared to the target position to gauge the individual point accuracy of the system and model. The results of this process are shown in Figure 6. This plot shows the positional error of the robot arm for each arm length tested and display how the final position differs from the desired target. Both of these tests display that some regions of the workspace fit the mathematical model well, while specific regions do have significant error. Despite these errors, these results display relatively high accuracy for a mathematical model describing a soft robot.

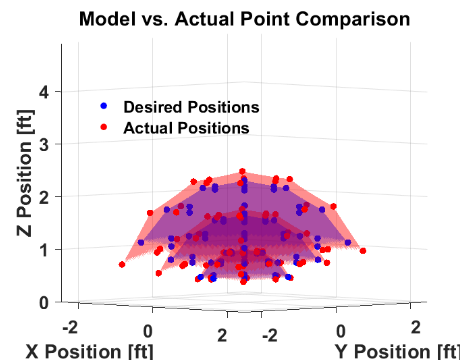

Figure 6. 3D positional data comparing desired positions to the actual position the model drove the robot to.

Response Time Testing: To test the system's response time, multiple points near the edge of the robot's workspace were chosen as target positions and the system drove to each of these points using the previously described controller. The system parameters response for one of these points is shown in Figure 7. These plots show the system parameters plotted over time as the robot moves from its default position to the desired target. The plots show that all system parameters follow comparable behaviors and reach their target values at approximately the same time. From these plots, an overall system rise time and settling time of 1.28 seconds and 3.30 seconds were found respectively. These times give a system response time of just over one second, which shows promising results for the goal of reaching a desired target within 2 seconds.

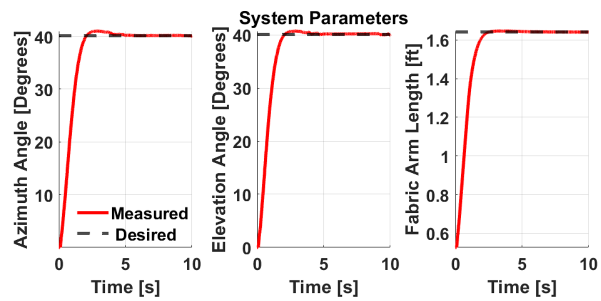

Figure 7. Plots of the system parameters (Azimuth, Elevation, and Fabric Arm Length) over time for a given test point.

System Control with Added Payload: To display the system's capability to navigate its workspace with a substantial payload, the system was driven to the same points from the response time testing but with the addition of a 1.21 lbs. payload. An example of the system's loaded behavior compared to its unloaded behavior is shown in Figure 8. These plots show that the added weight results in marginal overshooting increases for the azimuth angle and the fabric arm length. Otherwise, the plots display fairly comparable behavior for both the loaded and unloaded conditions. Thus, the system and its controller can compensate for added weight during operation despite the added weight not being accounted for in the controller's internal model. Therefore, the system can reliably operate with a minimum of 1.21 lbs. in the orchard environment. This shows promising results for the system's ability to work in the orchard and pick fruit.

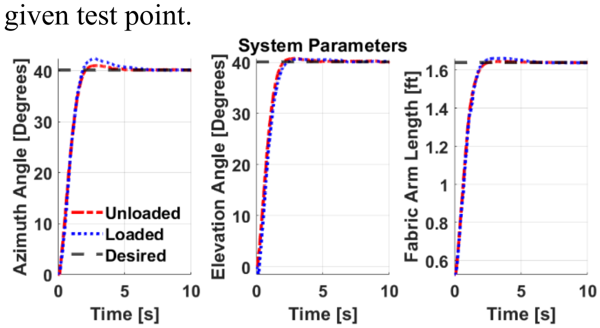

Figure 8. Plots of the system parameters (Azimuth, Elevation, and Fabric Arm Length) over time for with and without an added payload.

Teleoperation Control: Using the improved mathematical model, the system was controlled via teleoperation in both the lab and orchard environments, with the orchard setup being provided by Allan Bros. The in-lab tests showed no issues with navigating the lab testing space and simulated apple tree. The arm can reach multiple desired points around the tree whilst its base remained fixed. The in-orchard tests had comparable behavior despite the added challenges of operating the system in an outdoor environment. In both testing scenarios, the arm could rub against branches or apples without damaging the tree, fruit, or robot body. This was especially the case in the orchard test, as both the branches and the robot body deflected rather than cause damage to one another.

Results and Discussion:

Objective#1:

To improve the performance of our prior work, the design of the soft growing manipulator arm platform was iteratively improved upon. Specifically, several aspects were modified to enhance the steering performance, speed, and control. These changes are centered around the steering system. In particular, the steering collar and flexible buffer were redesigned, and a steering cable guide plate was introduced into the system. These changes improve the reliability of the system and increase the accuracy of the mathematical model. A diagram of the updated design is displayed in Figure 9. This design features the stronger fabric arm material and sealing, as well as the more potent central motor positioned externally to the pressurized enclosure from previous designs. The overall system is composed of four main components: the fabric arm, pressurized enclosure, steering system, and end-effector mount. The electrical system and the pressure regulation system are consistent with prior designs. Even with all of these changes, the overall cost of the robotic platform has not dramatically changed, at an estimated cost of $4,404.

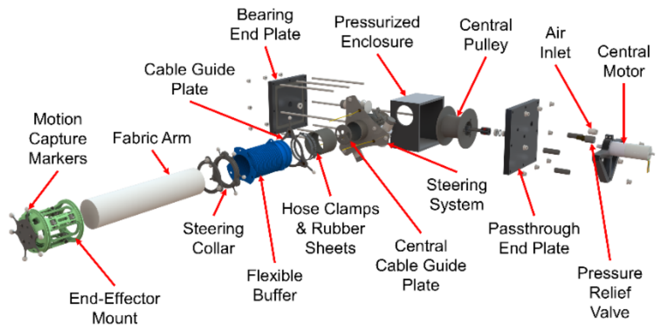

Figure 9. Exploded view of the current design of the soft growing manipulator platform with labels.

Pressurized Enclosure: The pressurized enclosure utilizes stock square aluminum extrusion and aluminum plates to reduce weight, machining time, and cost while maintaining the desired thickness. The two plates with rubber gaskets clamp on the open ends of the extrusion using threaded rods to create an airtight seal. A sanitary seal adapter is threaded to the front of the enclosure for mounting the steering system to the enclosure. The central motor is mounted externally resulting in a smaller enclosure size, as the only component inside is the central pulley. To maintain the safety and reliability of the enclosure there is a pressure relief valve, and the threaded rods are 3/8 inch fine threaded pressure vessel rated steel. The central motor has access to the central pulley through a rotary shaft pass-through hole with a mechanical seal to retain air pressure while allowing the shaft to freely rotate.

Fabric Arm: The arm has a diameter of 3.2 in and a length of 2.46 ft. The arm connects to the front of the system using hose clamps, and the central pully cable connects to the internal end of the fabric arm. The thick white thermoplastic polyurethane heat-sealable coating results in strong and reliable heat-seals without drastically impacting the weight or compliant nature of the fabric arm. The coating also makes the arm resilient to damage from its surroundings and water resistant.

Steering System: The steering system connects to the front of the pressurized enclosure using a clamping mechanism sourced from a sanitary seal, allowing the steering system to be adjusted as needed or removed entirely. The steering system is composed of three motors and pulleys mounted onto a steel plate, which use cables connected to the fabric arm via the steering collar to steer the arm, shown in Figure 10. The steering collar has been updated to provide better mounting location for the steering cables. The steering motors are oriented in a delta configuration with one motor's pulley oriented completely vertically. This configuration allows the system to counteract the effects of gravity on the fabric arm. An important change is the modification of the flexible buffer that covers the region of the fabric arm in between the steel plate and the steering collar. The buffer still holds extra fabric in a consistent shape allowing the steering region to extend and contract consistently. However, the new design is longer and stiffer, which greatly increases the system's steering range and reliability. This design also features grooves for the steering collar and cable guide plate. The last major change is the introduction of the cable guide plate which limits the movement and position of the steering cables making the system control more predictable and in-line with the mathematical model.

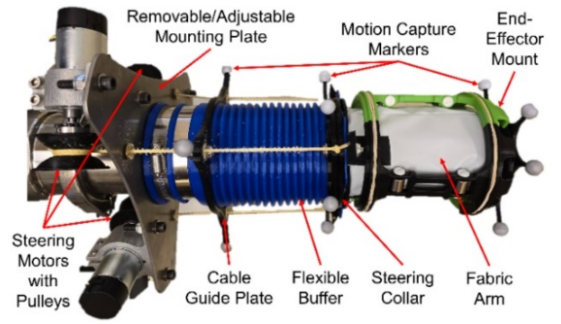

Figure 10. Picture of the steering system design with major components labeled.

End-effector Mount: The end effector mount is designed to reduce impedance during extension and retraction, as shown in Figure 11. The mount achieves this low friction due to the smaller diameter of the inner shell, the larger diameter of the outer shell, and the usage of roller magnets used to connect the two shells. The roller magnets are able to interact due to the inner shell magnets being connected to the shell via free-moving rails that side in and out radially. The outer shell is split into three sections held together via rubber bands. This design allows the outer shell to vary in diameter as the fabric arm slightly stretches while pressurized. This design significantly reduces the impedance by limiting the pinching one the fabric arm done by the mount without drastically increasing the weight. The entire mount is still lightweight at only 0.61 lbs.

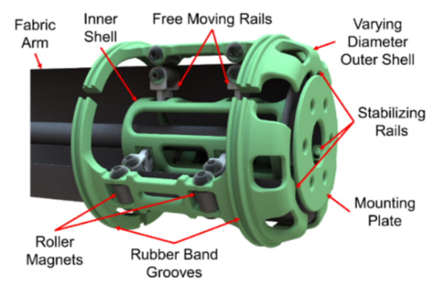

Figure 11. The end-effector mount with all major components labeled.

Objective#2:

Camera Selection: For our vision system, we utilize two RGBD cameras, one global camera, and one local camera on the end-effector of our soft robotic manipulator. The global camera is an Intel RealSense 435i camera and is used to detect all apples in robot's workspace. The local camera is an Intel RealSense 405 camera and is used to localize the tip of the robot and apples. The RealSense 435i's range of 1-10 ft is sufficient for this application due to the average width of the space between apple trees being approximately 7.54 ft across the aisle. Future work will incorporate a RealSense D456 as this model has a larger field of view and better weatherproofing. The RealSense 405 camera is a small and lightweight depth perception camera, that can be mounted into the palm of our soft gripper. The RealSense 405 camera ideal accurate reading range of 1.64 ft is appropriate for the end-effector camera as it will be used for fine-tuning the position of the end-effector towards its target through actuation.

Apple Detection Algorithm: A machine learning model (YOLOv8) was trained on a diverse set of apple orchard pictures collected from the Allan Brothers apple orchards in Prosser, WA. 3D pictures were taken in fair weather conditions (mostly sunny), and the RGB information was used to make labels for training and testing datasets. With this data, the model achieves a mean average precision value of 0.98 and a reasonable confidence percentage at >70% for detected apples. Currently, for the proof of concept, selecting a target apple is done by a user but future models will include an internal decision model to plan out the optimal order of apples to harvest. On top of apple detection, we have additional code that utilizes the RGBD information from the cameras to provide the 3D position of the apples with respects to the robot. This information is used to compute the error vector that is then used in the controller to perform manipulation.

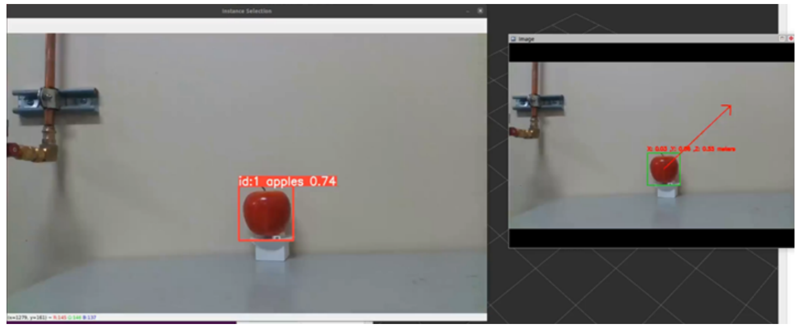

Figure 12. Images of the vision system detecting an apple and calculating the error vector used to drive the system.

Visual Servoing: Once the desired apple comes into the field of view of local camera, the system switches to segment based visual servoing using the local camera's feed. An error vector is calculated between the apple and center of the camera's view, shown in Figure 12. The controller then moves the manipulator to minimize the error. The vision-based position estimation through camera was accurate up to 0.98 in for each camera. The final deviation in the end effector position based on 15 different points was 0.91 in. Since the arm was not manipulated using the feedback of the vision system, system level accuracy cannot be determined as of now.

Image Based Localization: The apple detection YOLOv8 algorithm is incorporated into the end-effector localization by using the detected apples as points of interest. The algorithm is used to detect apples in local and global cameras' views and then the correlation between respective apples is found to calculate the respective displacement between cameras. Figure 13 shows the error bar of current experimental verification. The recorded error ranges from -3° to +3.2° in yaw and -0.51 to +1.34 inches in the yaw direction, and -3° to +2.2° and -0.28 to +1.26 inches in the pitch direction. A system comprised of two linear actuators is being constructed to determine the effect of motion blur on the efficacy of apple detection and displacement measurements between cameras by way of varying the parallel and perpendicular distance of the end-effector camera with respect to the row of apple trees. The displacement is directly correlated to the end-effector location, as the global camera is at a fixed position with respect to the body of the manipulator. The ongoing investigation towards the effect of motion parallel to the tree (continuous driving) is underway with a smaller, linearized testing structure to imitate the linear motion of the manipulator down a row.

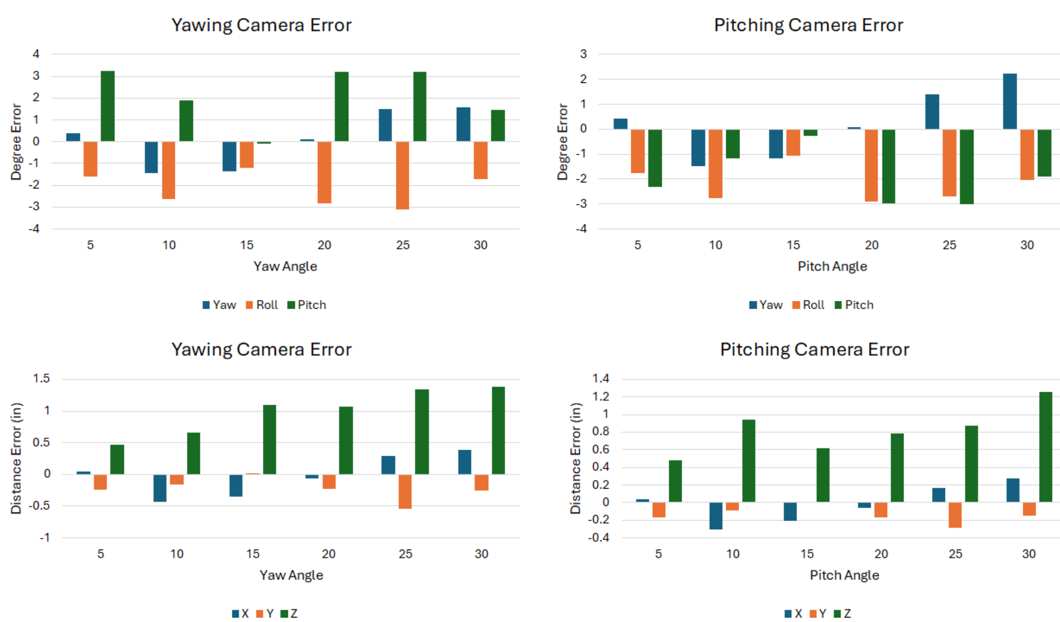

Figure 13. Error associated with pitch and yaw angle changes relative to row of apple trees.

Design and Results of the Soft Robotic Gripper: To overcome the shortcomings of the previous designs, our soft gripper end-effector has gone through multiple redesigns to improve harvesting efficiency. The current design uses fingers made from silicone rubber with a flexible 3D printed TPU embedded skeleton to increase the finger rigidity and force produced at the tip of the fingers. Cables running from the fingertips to a pulley connected to a servo motor cause the fingers to collapse inwards, allowing them to fully wrap around the apple when triggered. Previous pulley designs were fragile and too complex to repair in an orchard environment. To address this issue, the pulley design was simplified to reduce repair time and increase lifetime. To detect apples, the gripper has a limit switch located in the center of the palm. Future iterations will utilize the local camera for apple detection. Once the center switch is triggered, the servo motor rotates the pulley, creating tension in the cables and a moment at the tip of the fingers, bending them inwards and fully wrapping around the apple. The bottom limit switch is used for testing purposes to release the tension in the cables when pressed. A second servo was added to the base along with a gear system so that the entire gripper can twist after it has grasped an apple, shown in Figure 14. This twisting motion simulates how a human worker picks an apple. The gripper weighs approximately 0.91 lbs., thereby meeting the payload requirements. From testing three different internal skeletons in the field, the top performing gripper yielded a successful harvesting rate of 87%, as seen in Figure 15. Future work will involve the testing and verification of the twisting motion gripper while integrating onto the robot platform and vision system to complete automated harvesting experiments.

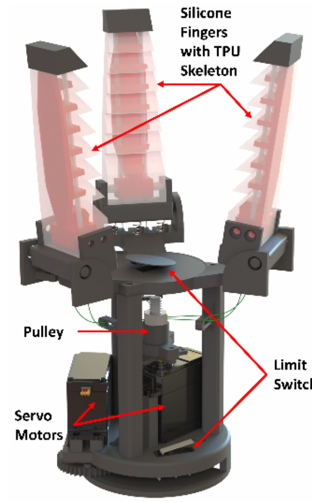

Figure 14. Soft robotic gripper with twisting mechanism.

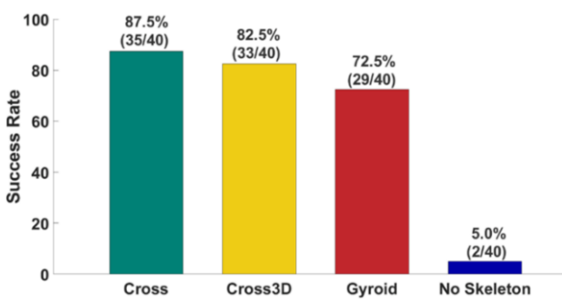

Figure 15. Rate of successful picks for each of the gripper types.

Objective#3:

Mathematical Model: With all the iterative improvements and design changes to the structure of the robotic platform, a new mathematical model of the system was created. This model uses the previous mathematical models as a basis and considers how each motor impacts each of the system parameters. The updated model provides a vastly more accurate depiction of the physical system, which makes the control and movement planning of the robotic platform simpler and faster to compute and execute.

Controller: To determine the best control method for the new system and mathematical model, multiple controller designs were implemented and then compared to one another. After extensive testing a model reference adaptive controller design was chosen to be the main controller of this system. This controller utilizes data collected from the physical system to make the system parameters follow a desired reference model as closely as possible. Using this design provides a high degree of repeatability and guarantees stability. Enabling the system to accurately reach a desired position within a short amount of time while reducing the total distance traveled. This controller also allows for simple implementation with the machine vision systems, as it only requires knowing the position of the end-effector.

Executive Summary:

One of the major pressing issues facing Washington State tree fruit growers is the sourcing of adequate labor for critical operations such as harvesting and pruning. To address this issue, many growers and groups have invested in the development of labor-saving technologies like robotics. In particular, there has been great interest in the research and implementation of tree fruit harvesting and pruning robots. Our work has contributed to this growing field by introducing a novel soft growing manipulator arm platform to the orchard environment. This soft-robotic platform has been designed to accomplish automated orchard operations while being safe for the trees and fruit as well as being low-cost. Specifically, the platform uses a low-inertia fabric body and a lightweight soft-gripper harvesting end-effector resulting in a prototyping cost of $4,404 for a single manipulator. The soft-gripper end-effector has soft silicone rubber and flexible plastic fingers to handle fruit in a safe and consistent manner. The system also utilizes a multi-faceted machine vision camera system to detect the 3D position of apples and the position of the manipulator arm, allowing the system to drive the arm to a desired point. This vision system utilizes a global camera mounted on the enclosure of the manipulator and a local camera mounted onto the end-effector. Currently, the end-effector positioning system uses a QR code mounted on the end-effector, but future work aims to incorporate the image-based localization system that is under development. To control the manipulator arm, a mathematical model was developed to describe the physical system. With this model, a Model Reference Adaptive Controller (MRAC) was designed and implemented into the system to achieve a desired control behavior and to guarantee stability. The performance capabilities of the manipulator arm were determined and characterized in the lab setting using a series of tests. From these tests, the arm was found to have the following performance metrics: a 2.46 ft maximum controllable arm length, a 1.23 ft/s extension speed and 0.86 ft/s retraction speed at 8 and 3 psi respectively, a maximum payload of 2.39 lbs. at its max arm length, a spherical sector-shaped workspace with a volume of 22.46 ft^3, and operating pressures between 5 and 10 psi. The apple detection system has been validated in the lab and orchard environments and found to have a mean average precision value of 0.98 and a confidence percentage of >70% for detected apples. The current and under development localization systems have been tested in the lab environment with maximum positional errors less than 1.34 in. However, further work is being done to validate and improve the accuracy of these system as well as test them in an orchard setting. Various versions of the soft-gripper end-effector were tested in a commercial apple orchard provided by Allan Brother's Orchard during the 2023 harvesting season, with the best performing gripper having an 87.5% successful pick rate. The mathematical model of the system was validated through two tests that compared the actual positions to the positions the model drove the system to. From these tests, the model was found to be relatively accurate for a soft robotic system. Then the MRAC was tested with and without an additional 1.21 lbs. payload to determine the system's response time and its ability to compensate for additional payloads. The first test displayed an overall system rise time and settling time of 1.28 seconds and 3.30 seconds respectively for a point near the boundary of the system's workspace. The second test demonstrated the system's ability to compensate for added payloads with marginal differences in performance metrics. Finally, the system was teleoperated controlled in a commercial apple orchard to demonstrate the system's ability to navigate the complex orchard environment without damaging the trees, fruit, or itself. Future work will focus on upgrading and integrating the machine vision camera system with the soft-gripper end-effector and the manipulator arm, and then conducting in-orchard harvesting experiments to analyze the robot's ability to conduct orchard operations.